Inorganic Chemistry
Article
pubs.acs.org/IC

Dual Application of (Aqua)(Chlorido)(Porphyrinato)Chromium(III) as Hypersensitive Amine-Triggered ON Switch and for Dioxygen Activation

Philip Heier,[†,‡] Nicolas D. Boscher,[‡] Patrick Choquet,[‡] and Katja Heinze*,[†]

[†]Institute of Inorganic and Analytical Chemistry, Johannes Gutenberg University of Mainz, D-55128 Mainz, Germany
[‡]Science and Analysis of Materials Department, Centre de Recherche Public-Gabriel Lippmann, L-4422 Belvaux, Luxembourg

S *Supporting Information*

ABSTRACT: Although synthesis and substitution reactions of chlorido chromium(III) porphyrins $Cr^{III}(TPP)(Cl)(L)$ (H_2TPP = 5,10,15,20-tetraphenyl porphyrin, L = pyridine, H_2O, ROH, etc.), have been well-established in coordination chemistry for decades, an unexpected dichotomous reactivity of $Cr^{III}(TPP)(Cl)(H_2O)$ (**1**) toward amines is disclosed here. This reactivity leads to the application of **1** as highly sensitive substoichiometric and irreversible ON switch for amine detection by an autocatalytic pathway. The concomitant activation of O_2 by the **1**/amine system is furthermore exploited in an electrochemically driven epoxidation of norbonene using O_2 as initial oxidant.

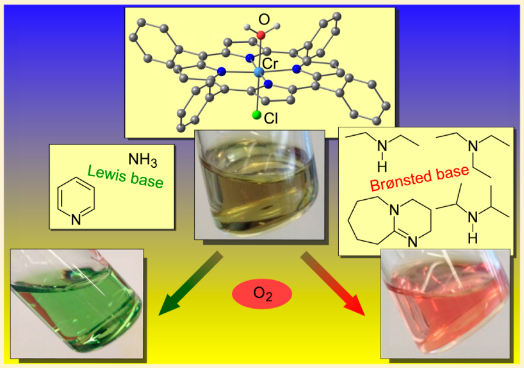

INTRODUCTION

Chromium porphyrins were introduced in 1966 by Tsutsui and co-workers with the synthesis of chromium(II) and chromium(III) mesoporphyrin IX dimethyl ester.[1,2] Shortly after, the preparation of chromium *meso*-tetraphenyl porphyrins from H_2TPP and $CrCl_2$ in dimethyl formamide was reported by Adler et al. (Scheme 1),[3] and an optimized aqueous purification procedure was subsequently developed by Summerville et al. in 1977.[4]

The initially formed chromium(III) porphyrin complex is considered to be the five-coordinate $Cr^{III}(TPP)(Cl)$ complex, which readily coordinates a sixth ligand L to form the respective stable six-coordinate octahedral $Cr^{III}(TPP)(Cl)(L)$ complex **2**. Generally, the Cr^{III} ion cannot be easily removed from the porphyrin macrocycle except upon exposure to strong mineral acids.[5] Members of the $Cr^{III}(TPP)(Cl)(L)$ family have been thoroughly analyzed by cyclic voltametry,[6−8] electron paramagnetic resonance (EPR),[4,9] and emission[10,11] and UV−vis spectroscopy.[4,11,12] All complexes show characteristic porphyrin absorptions with the intense Soret band at ~445−460 nm and the weaker Q bands at ~500−610 nm. Chromium(III) porphyrins show additional absorptions in the near-UV as well as in the near-IR region and have been classified as d-type hyperporphyrins.[11,13] The exact energy of the porphyrin absorption band strongly depends on the nature of the sixth ligand L.

Scheme 1. Synthesis and Reactivity of 1

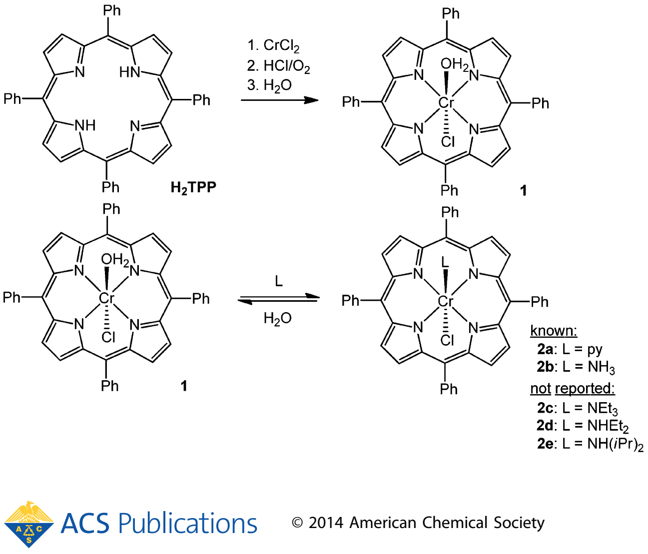

As shown in 1995, the commonly employed synthetic procedure described by Summerville,[4] which includes an aqueous workup, yields the aqua complex $Cr^{III}(TPP)(Cl)(H_2O)$ (**1**).[14] The axial water ligand can easily be substituted by other ligands L such as pyridine or ammonia (Scheme 1, **2a** or **2b**) as axial ligand exchange in chromium(III) porphyrins is reported to be up to 10^4 times faster compared to other chromium(III) complexes.[15,16] Substitution by several pyridine derivatives occurs in a dissociative manner via the five-coordinate intermediate $Cr^{III}(TPP)(Cl)$.[17] This intermediate is also generated photochemically by laser photolysis, which has advanced further kinetic studies.[14,18,19] Even though a direct

Received: July 11, 2014
Published: October 1, 2014

© 2014 American Chemical Society

comparison of all available studies dealing with thermal or photoinitiated ligand exchange is difficult, a general trend for the affinity of $Cr^{III}(TPP)(Cl)$ toward different donor atoms has been extracted by Hoffman and Basolo, which follows the order $N \gg P > O \approx S$.[4,5] In the absence of steric restrictions, the affinity of chromium(III) porphyrins toward nitrogen donor ligands increases as the pK_b of the ligand decreases.[12] For example, the binding constant of $Cr^{III}(TPP)(Cl)$ for pyridine (pK_b = 8.73) in dichloromethane is reported to be $K = 1.9 \times 10^5$ M^{-1} while *sec*-butylamine (pK_b = 3.44) binds 3.5 times stronger ($K = 6.6 \times 10^5$ M^{-1}).[12] The properties of $Cr^{III}(TPP)(Cl)(L)$ porphyrins **1** and **2** suggest their application as colorimetric amine sensors for the following reasons: (a) the complexes show intense absorptions in the visible spectral region that are strongly dependent on the coordinated sixth ligand L; (b) they display a very high affinity for nitrogen-containing ligands and discriminate them from phosphorus, oxygen, and sulfur-based ones, and (c) in contrast to zinc(II) porphyrins often employed in amine sensing,[20−24] the Cr^{III}(porphyrinato) core is exceptionally stable toward acidic and basic conditions. Hence, we had developed sensing devices[25] for volatile amines based on Cr^{III}(porphyrinato) complexes applicable to the control of food freshness in easy-to-use packaging foils.[26−28] Interestingly, the employed (aqua)(chlorido)(porphyrinato)chromium(III) complexes feature an unexpected pronounced hypsochromic shift of the Soret and Q bands in the reaction with NEt_3 as a prototypical volatile amine. Furthermore, the reaction with NEt_3 is irreversible, a rather unusual finding for a simple O-donor to N-donor ligand substitution.[4,12]

Here we disclose the puzzling reactivity and unusual color change of **1** treated with triethylamine and other N-donor ligands in solution. The distinct mechanism, which opens a novel "green" pathway to oxido chromium(IV) porphyrins, is clarified, and applications in the fields of amine sensing and aerobic alkene epoxidation[29] are discussed.

■ RESULTS AND DISCUSSION

The aqua complex **1** was prepared according to the literature from $CrCl_2$ and H_2TPP giving intermediate Cr(TPP) (**3**) and its subsequent aeral oxidation to **1**.[4,14,19] Its correct formation is corroborated by field desorption (FD) and electrospray ionization (ESI) mass spectrometry (MS) (m/z = 682.18 $[M-Cl]^+$; m/z = 699.14 $[M-H_2O]^+$; Supporting Information, Figure S1). The UV−vis absorption spectrum of **1** in CH_2Cl_2 shown in Figure 1a (black curve) fully conforms to literature data.[4] The olive-green colored solution exhibits a strong Soret band at 448 nm, Q-band absorptions at 563 and 603 nm, and a quite prominent ligand-to-metal charge transfer band at 396 nm (Figure 1a). Exposure of this solution to excess pyridine (py) leads to the expected formation of $Cr^{III}(TPP)(Cl)(py)$ (**2a**) and a rather unremarkable color change to grass-green (Figure 1b). This is caused by the expected bathochromic shift of the absorption bands to 458 nm (Soret band) and to 572/610 nm (Q bands), respectively (Figure 1, dashed green curve). As bathochromic shifts are typically observed for substitutions of oxygen donor ligands by nitrogen donors at chromium(III) porphyrins,[4,12] this observation corresponds well to values reported in the literature for the aqua-to-pyridine ligand substitution in toluene[4] or in CH_2Cl_2.[12]

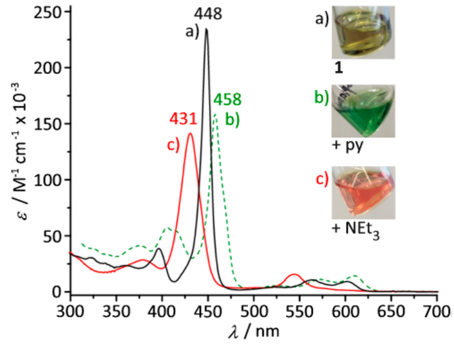

Figure 1. . UV−vis absorption spectra in CH_2Cl_2 of (a) **1** (black), (b) **1** with excess pyridine (dashed green), and (c) **1** with excess NEt_3 (red). (inset) Photographs of the respective solutions.

Fully unexpected, a solution of **1** in CH_2Cl_2 turns bright red in the presence of triethylamine. Hypsochromic shifts are observed with the Soret band at 431 nm, the Q-band at 544 nm, and the ligand-to-metal charge transfer band at ∼380 nm (Figure 1c). This observation suggests that a different complex is formed instead of the expected substitution product $Cr^{III}(TPP)(Cl)(NEt_3)$ (**2c**) (Scheme 1).

UV−vis, IR, and ^1H NMR analyses of the resulting red solution clearly suggest that the diamagnetic oxido chromium(IV) complex $Cr^{IV}(TPP)(O)$ (**4**) was formed quantitatively (Scheme 2 and Supporting Information, Figures S2 and S3).[30−33] The oxido complex **4** has been previously prepared by aerobic oxidation of the chromium(II) complex **3**,[30,32] by oxygenation of **1** with strong oxygen atom transfer reagents (iodosylbenzene,[31,34,35] *meta*-chloroperoxybenzoic acid (MCPBA),[35] sodium hypochlorite,[36] *tert*-butyl hydroperoxide,[34] *p*-cyano-*N*,*N*-dimethylaniline *N*-oxide/photoexcitation[37]), and via aerobic oxidation under acidic (HCl) conditions and subsequent basic workup possibly via a dichlorido intermediate $\mathbf{5}^-$ and its porphyrin radical cation complex **5**[30] (Scheme 2). To the best of our knowledge, formation of the oxido chromium(IV) complex **4** by amines under ambient conditions (humid air) has not yet been

Scheme 2. Known Routes to Cr^{IV} Complex 4

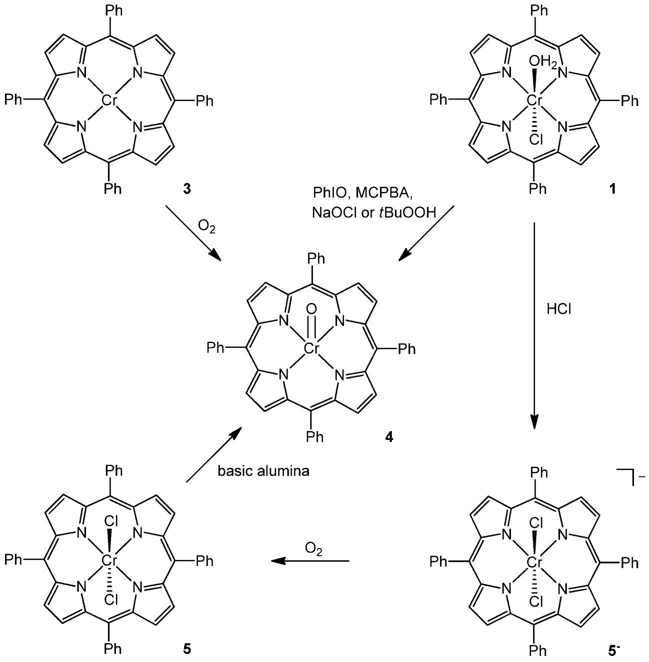

reported. Interestingly, Cr^{V}(corrolato)(O) complexes have been directly obtained from free-base corrole, $Cr(CO)_6$, and O_2, showing that corroles stabilize high metal oxidation states.[38] The only feasible oxidant in the present reaction scheme **1**/NEt_3 is dioxygen as well. However, as the chromium(III) complex **1** itself is completely inert toward dioxygen the amine obviously activates **1** prior to the oxidation by O_2. As the reaction with O_2 also occurs in the absence of light a photochemical pathway such as found for an (octakis(*p*-*tert*-butylphenyl)-corrolazinato)manganese(III) complex[39] is excluded.

A possible first route requires an initial reduction of Cr^{III} to Cr^{II} (**3**) by the amine and further reaction of the Cr^{II} complex **3** with O_2 corresponding to a reductive activation by electron transfer. A second possible pathway occurs via a hydroxido complex $[Cr^{III}(TPP)(OH)(Cl)]^-$ (**6**$^-$) obtained by proton transfer. To observe the initially formed active species in this complex reaction scheme **1** → **4** we first investigated the reaction of **1** with NEt_3 in the absence of dioxygen.

Reaction of 1 with NEt_3 in the Absence of Dioxygen. Chromium(III) porphyrin **1** is treated with 0.5 equiv, 1.0 equiv, or excess of NEt_3 in CH_2Cl_2 under exlusion of O_2, and the respective UV−vis spectra are depicted in Figure 2.

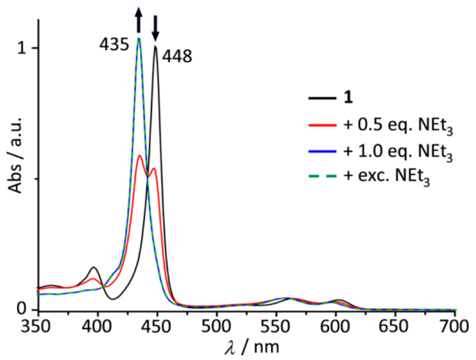

Figure 2. UV/vis absorption spectra of **1** in CH_2Cl_2 under Ar atmosphere; (a) **1** (black, solid) and after the addition of (b) 0.5 equiv of NEt_3 (red, solid), (c) 1.0 equiv of NEt_3 (dark blue, solid) and (d) excess of NEt_3 (green, dashed).

The absorption bands of **1** are replaced by new bands at higher energies, their intensities being proportional to the amount of added NEt_3 with a quantitative conversion accomplished with 1 equiv of NEt_3. An excess of NEt_3 does not further change the spectrum. The charge-transfer band ~396 nm is diminished, the Soret band is shifted from 448 to 435 nm, and the Q bands are shifted from 563 to 557 nm and from 603 to 596 nm, respectively. These spectral data differ from those of **4** and pyridine complex **2a** suggesting neither oxidation of **1** nor substitution of the H_2O ligand by NEt_3. Isosbestic points at 404, 442, and 562 nm indicate a clean reaction without observable intermediates. A similar spectral behavior of chromium(III) porphyrins has been described in the literature for the substitution of a chlorido ligand by an alkoxido ligand.[40] In the present case this either indicates deprotonation of the aqua ligand by NEt_3 giving $[Cr^{III}(TPP)(OH)(Cl)]^-$ (**6**$^-$) and subsequent substitution of the chlorido ligand by H_2O to form $Cr^{III}(TPP)(OH)(H_2O)$ (**7**)[41] or direct substitution of the chlorido ligand of **1** by hydroxide (**7**). The latter reaction might be less favorable as the aqua ligand in **1** is only weakly trans-activating. The formation of hydroxido complexes (**6**$^-$, **7**) is further supported by the reaction of **1** with LiOH. Treatment of **1** with a deoxygenated solution of LiOH in CH_2Cl_2 results in exactly the same absorption spectrum as that of the addition of NEt_3 to **1** (Figure 3). Subsequent exposure of both solutions to air results in the slow formation of **4**.

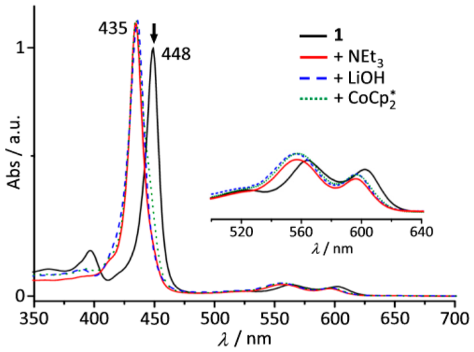

Figure 3. UV−vis absorption spectra in CH_2Cl_2 under Ar atmosphere of (a) **1** (solid black curve), (b) **1** with 1 equiv of NEt_3 (solid red curve), (c) **1** with excess of LiOH (dashed blue curve), and (d) **1** with 1 equiv of $CoCp^*_2$ (dotted green curve). (inset) Magnifications of the Q-band region.

No Cr^{II}(TPP) intermediate **3** with its characteristic Soret band at 420 nm[42,43] is observed by UV−vis spectroscopy after addition of NEt_3 or OH^- to **1**. Attempts to chemically reduce the aqua complex **1** to **3** by 1 equiv of decamethylcobaltocene $CoCp^*_2$ ($E_{1/2}$ = −1.94 V in CH_2Cl_2 vs ferrocene/ferrocenium)[44] only resulted in the formation of **6**$^-$/**7** instead of Cr^{II}(TPP), as seen from the absorption spectrum in Figure 3 (dotted green curve; minor differences in the near-UV region result from $[CoCp^*_2]^+$ absorptions). We ascribe this observation to proton reduction by $CoCp^*_2$[45] resulting in a net deprotonation of **1** as observed for the reactions of **1** with NEt_3 or with OH^-. Hence, a reductively initiated pathway via **3** seems unlikely. Furthermore, the redox potential of NEt_3 ($E_{1/2}$ = 0.47 V in CH_3CN vs ferrocene/ferrocenium)[44] is insufficient to reduce **1** (E_p = −1.33 V; irreversible; Cr^{III} → Cr^{II}).[46] In fact, the cyclic and square-wave voltammetric data confirm that the Cr^{III} → Cr^{II} reduction is even more difficult in the presence of LiOH (E_p = −1.54 V; irreversible; Cr^{III} → Cr^{II}) (Supporting Information, Figure S4). This is in good agreement with the proposed formation of hydroxido complexes **6**$^-$ and/or **7**. The assignment is furthermore consistent with results published for Cr^{III}(OEP)(Cl) complexes (OEP = octaethylporphyrin) showing a 0.26 V shift by chlorido-to-hydroxido substitution in dimethylsulfoxide.[6,34] First and second reversible oxidations to the porphyrin radical cation and the porphyrin dication are slightly affected by the presence of LiOH (Supporting Information, Figure S4). The first wave shifts from 0.44 to 0.41 V, and the second one shifts from 0.93 to 0.91 V. A weak wave around 0.17 V is assigned to the oxidation of chloride ($E_{1/2}$ = 0.18 V in CH_3CN vs ferrocene/ferrocenium).[44] In summary all spectroscopic evidence points to the presence of hydroxido complexes **6**$^-$ and/or **7** in the presence of NEt_3 or LiOH under anaerobic conditions.

DFT Studies on the Reaction of 1 with NEt_3. The conceivable reaction products of **1** with NEt_3 have been studied by density functional calculations (B3LYP, LANL2DZ, iefpcm model for CH_2Cl_2; Figure 4),[47] and selected metrical data are

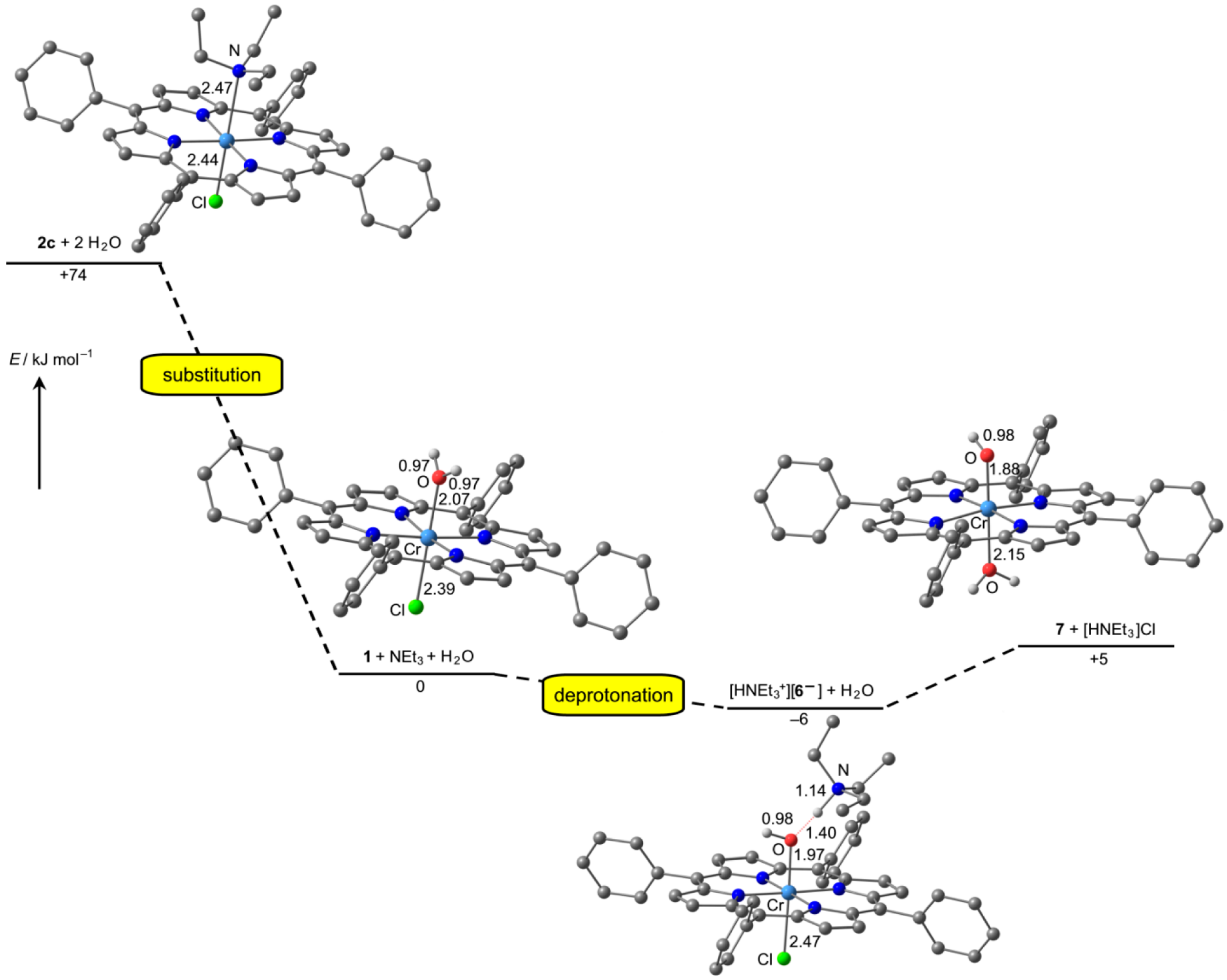

Figure 4. DFT (B3LYP, LANL2DZ, iefpcm model for CH_2Cl_2) optimized structures and relative thermal energies of **1**+NEt_3+H_2O; **2c**+2H_2O, [$HNEt_3^+$][**6**$^-$]+H_2O, and **7**+$HNEt_3Cl$. CH hydrogen atoms are omitted for clarity. Distances are given in Å; energies are given in kJ mol^{-1}.

Table 1. Selected Bond Lengths [Å] and Angles [deg] of 1 in the Solid State[14] and as Derived from DFT Calculations

	1 (XRD)[a]	**1** (DFT)[b]	[$HNEt_3^+$][**6**$^-$][c]	**7**	**2c**
	X = Cl	X = Cl	X = Cl	X = OH	X = Cl
	L = H_2O	L = H_2O	L = HO···H	L = H_2O	L = NEt_3
Cr−X	2.242(3)	2.388	2.474	1.883	2.436
Cr−L	2.239(3)	2.066	1.967	2.148	2.471
Cr−N(porph)[c]	2.031(2)	2.051[d]	2.057[d]	2.060	2.049
O−H		0.974/0.974	0.978/1.396	0.981	
H−N			1.144		
X−Cr−L	180.0	179.9	178.1	179.3	178.1
X−Cr−N(porph)[c]	89.0(1)	92.3	90.0	93.2	89.0
L−Cr−N(porph)[c]	91.0(1)	87.7	90.0	86.8	91.0
out-of-plane distance					
Cr−porph	0.035 to X	0.073 to X	0.018 to L	0.109 to X	0.119 to L
D_{oop}[d]		0.1316	0.1608	0.1504	0.4638
E/kJ mol^{-1}		0	−6	+5	+74

[a]From ref 14. [b](B3LYP, LANL2DZ, iefpcm model for CH_2Cl_2) for **1**+NEt_3+H_2O, [$HNEt_3$][**6**$^-$]+H_2O, **7**+[$HNEt_3$]Cl, and **2c**+2H_2O. [c]Values averaged for the four nitrogen atoms of the porphyrin. [d]Total out-of-plane distortions as obtained from normal structural decomposition (NSD)[48] analyses.

summarized in Table 1. Substitution of the aqua ligand by NEt_3 to give **2c** is calculated to be thermodynamically disfavored by 74 kJ mol^{-1} (Figure 4, Table 1). The normal coordinate analysis of the porphyrin deformation (normal structural decomposition (NSD))[48] and the derived total out-of-plane distortion D_{oop} of the porphyrin clearly reveal a rather strong distortion of the porphyrin due to the NEt_3 coordination. This is also reflected in the out-of-plane displacement of the chromium toward the amine (Table 1). All these distortions imposed by the steric bulk might account for the low stability of the NEt_3 complex **2c**.

On the other hand, attack of NEt_3 at the aqua ligand of **1** gives the hydroxido complex $\mathbf{6}^-$ with an asymmetric hydrogen bond to the ammonium ion; hence, a hydrogen-bonded contact ion pair $[HNEt_3^+][\mathbf{6}^-]$ is formed (Figure 4). This proton transfer is thermodynamically favorable by 6 kJ mol^{-1}. Almost isoenergetic to hydrogen-bonded $\mathbf{6}^-$ is the neutral (aqua)(hydroxido)chromium(III) complex **7** and triethylammonium chloride (Figure 4). Complex **7** might be easily formed from $\mathbf{6}^-$ due to the stronger trans influence of OH^- ($\mathbf{6}^-$: Cr−Cl 2.47 Å) as compared to H_2O (**1**: Cr−Cl 2.39 Å) labilizing the Cr−Cl bond. Hence, both complexes $\mathbf{6}^-$ and **7** should be in equilibrium in alkaline solution. Especially the anionic complex $\mathbf{6}^-$ might be susceptible toward oxidation by O_2 similar to the reactivity of the proposed dichlorido intermediate $\mathbf{5}^-$.[30] Formation of electron-rich anionic Cr^{III} complexes is thus likely the key factor for the oxidation of **1** with dioxygen as no reaction of **1** with O_2 is observed in the absence of OH^- or Cl^-.

Reaction of 1 with other Nitrogenous Bases. As the results presented so far indicate that H_2O ligand substitution does not occur at **1** with NEt_3 but that NEt_3 acts as a Brønsted base instead, different nitrogen-based ligands of different basicity and steric demand were investigated. The results are compiled in Scheme 3.

Scheme 3. Dichotomous Reactivity of 1 with Potential N Ligands under Ambient Conditions[a]

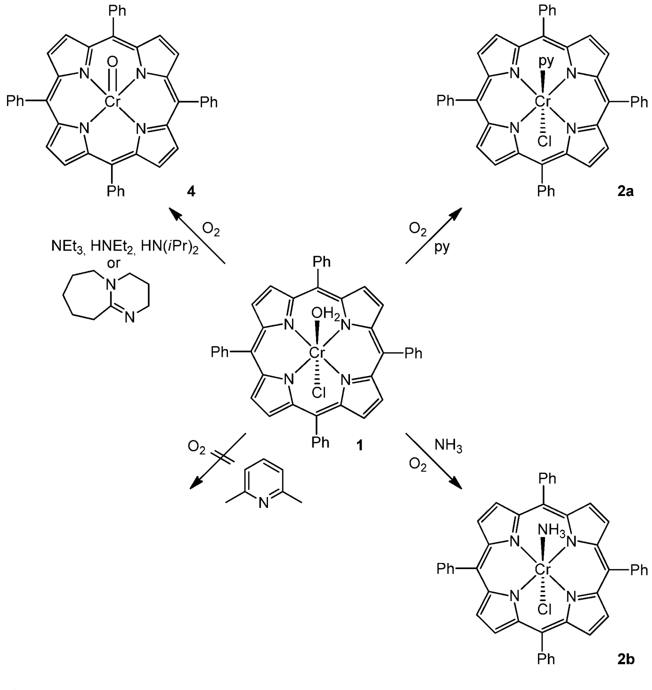

[a]py = pyridine.

The weak base pyridine (pK_b = 8.7[49a]) substitutes for the aqua ligand to give the pyridine complex **2a**.[12] Similarly, ammonia (pK_b = 4.8[49b]) yields the respective green ammine complex **2b** by ligand substitution (Supporting Information, Figure S5). The stronger bases NEt_3 (pK_b = 3.2[50]), $HNEt_2$ (pK_b = 3.0[50]), and $HN(^iPr)_2$ (pK_b = 2.9[50]) finally yield the red oxido chromium(IV) complex **4**. The same observation holds for the weakly coordinating but strong base 1,8-diazabicyclo[5.4.0]undec-7-ene (DBU, pK_b = 2.0[50]). On the other hand sterically demanding 2,6-lutidine (pK_b = 7.2[49a]) is neither competent to substitute nor to deprotonate the aqua ligand. As *sec*-butylamine (pK_b = 3.44) has been reported to coordinate to Cr^{III}[12] a clear reactivity borderline between ligand deprotonation (Brønsted acid/base reaction; $pK_b \leq 3.2$) and ligand substitution is obvious (Lewis acid/base reaction; $pK_b \geq 3.4$).

Reactions of Cr^{III}(TPP)(Cl)(THF) (8). To strengthen the conclusion that deprotonation of the aqua ligand in **1** is the key step in the conversion of **1** to **4** initiated by NEt_3 water-free Cr^{III}(TPP)(Cl)(THF) (**8**) was treated with NEt_3. The tetrahydrofuran (THF) complex **8** was prepared by dissolving **1** in THF and drying the solution with $CaCl_2$. The spectral data of **8** are in full accordance with literature values (Supporting Information, Figure S6).[4] Treating **8** with excess NEt_3 in THF under exclusion of dioxygen and water does not give any spectral changes (Supporting Information, Figure S6). Obviously NEt_3 is unable to replace THF in **8** to give **2c** in the presence of excess THF and even in anhydrous CH_2Cl_2. Dissolving **8** in CH_2Cl_2 under humid air and addition of NEt_3 forms **4** albeit much slower than in the reaction starting from **1**. Likely, the aqua complex **1** or the hydroxido complexes $\mathbf{6}^-/\mathbf{7}$ have to be formed first from **8**.

Reaction of 1 with Substoichiometric Amounts of NEt_3. All results described above were achieved using an excess of strong bases. This leads to a rapid conversion of **1** to **4** within minutes with a stable (irreversible) absorption shift. The distinct absorption changes, which are clearly visible to the naked eye (Figure 1), had suggested the use of **1** incorporated in a porous matrix[26−28] as a colorimetric sensor for basic volatile amines[21−24,50] for the control of food freshness.[51−53] To determine the detection limit **1** was treated with stoichiometric and substoichiometric amounts of NEt_3.

Figure 5a shows the temporal evolution of the UV−vis spectra of a solution of **1** in CH_2Cl_2 after addition of 1 equiv of NEt_3. Under these conditions quantitative conversion of **1** to **4** is achieved in 60−90 min (red line). No isosbestic points are found indicating the accumulation of intermediates. This is in good agreement with the deprotonation/oxidation pathway described above. **1** is initially deprotonated by NEt_3 to form intermediate hydroxido complexes $\mathbf{6}^-/\mathbf{7}$ (λ_{Soret} = 435 nm), which are subsequently oxidized by O_2 to the final product **4** (λ_{Soret} = 431 nm). Unexpectedly, addition of 0.1 equiv of NEt_3 also lead to a quantitative conversion to **4** as shown in Figure 5b although this reaction is only completed after 14 h. For ease of comparison, the 90 min spectrum of this reaction still showing the presence of residual starting material is also plotted in Figure 5b (red curve).

The rate of the conversion of **1** to **4** depends on the solvent used. Reactions in nonpolar toluene (Figure 6a) are much faster as compared to reactions in more polar CH_2Cl_2 solutions (Figure 5b). As O_2 solubility is similar in both solvents[54] a simple concentration effect is not responsible. In toluene the reaction of **1** with 0.1 equiv of NEt_3 is already completed within 90 min instead of the 14 h required in CH_2Cl_2. Clean isosbestic points are observed in the UV−vis spectra for the reaction in toluene at 440 and 556 nm (Figure 6a). This indicates that the intermediate (presumably $\mathbf{6}^-/\mathbf{7}$) does not accumulate in toluene but is rapidly oxidized by O_2.

As the reaction of **1** with 0.1 equiv of NEt_3 in toluene is quantitative within a reasonable amount of time studies with even less amounts of NEt_3 were performed in toluene solution.

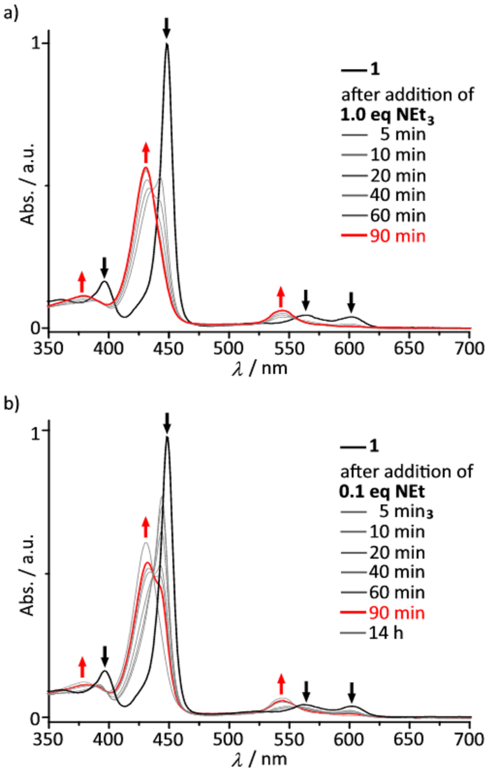

Figure 5. Temporal evolution of UV−vis absorption spectra of **1** in CH_2Cl_2 after addition of (a) 1.0 equiv of NEt_3 and (b) 0.1 equiv of NEt_3. Red curves represent spectra after 90 min.

Addition of 0.01 and 0.001 equiv of NEt_3 also lead to a distinct absorption change after 90 min as depicted in Figure 6b,c. In both cases conversion to **4** is not yet quantitative after 90 min, but it is obviously significantly larger than 1% or 0.1%, respectively, as would be expected for a stoichiometric reaction of **1** with NEt_3 to give **4**. From the spectra depicted in Figure 6b,c conversions of 79% and 63% (based on **1**) after 90 min are determined for the reaction of **1** with 0.01 and 0.001 equiv of NEt_3, respectively.

To interpret this observation we take a closer look at the net reaction of **1** to **4**. The initial step is the deprotonation of **1** to the intermediate $\mathbf{6}^-$ (Scheme 4, base-initialized pathway), which is subsequently oxidized to **4** by O_2. In the net reaction one chloride ion and one proton per chromium(III) porphyrin **1** is released apart from H_2O formation. So far no details concerning the oxidation mechanism, specifically, whether the oxido ligand in **4** originates from water or from dioxygen, are known. This will be addressed in future studies. From the literature it is known that HCl can induce the autoxidation of **1** to **4** presumably via the dichlorido complex $\mathbf{5}^-$ (Scheme 4, chloride-initiated pathway).[30] Hence, only a small amount of base (either strong nitrogenous bases or LiOH) is initially required as one of the products, namely, the chloride ion, also induces the transformation. This amplification by a product is a typical autocatalytic process.

To confirm the proposed chloride effect, a solution of **1** in CH_2Cl_2 was treated with excess LiCl. Analysis of the resulting UV−vis spectra over time shows that **1** is indeed slowly converted to **4** under these conditions indicating the formation of the dichlorido complex $\mathbf{5}^-$, which is subsequently oxidized to **4** (Supporting Information, Figure S7). This result confirms the chloride-initiated pathway from **1** to **4** depicted in the lower part of Scheme 4. Combination of both pathways explains the hyper-stoichiometric conversion observed with respect to NEt_3. The initially inert chromium(III) complex **1** is deprotonated by the amine generating the reactive intermediate $\mathbf{6}^-$, which is oxidized by dioxygen to give **4** and chloride. During that reaction the base is consumed, but chloride accumulates stoichiometrically opening a second activation pathway of **1** via the formation of $\mathbf{5}^-$. This autocatalytic reaction finally results in a slow, yet full conversion of **1** to **4**.

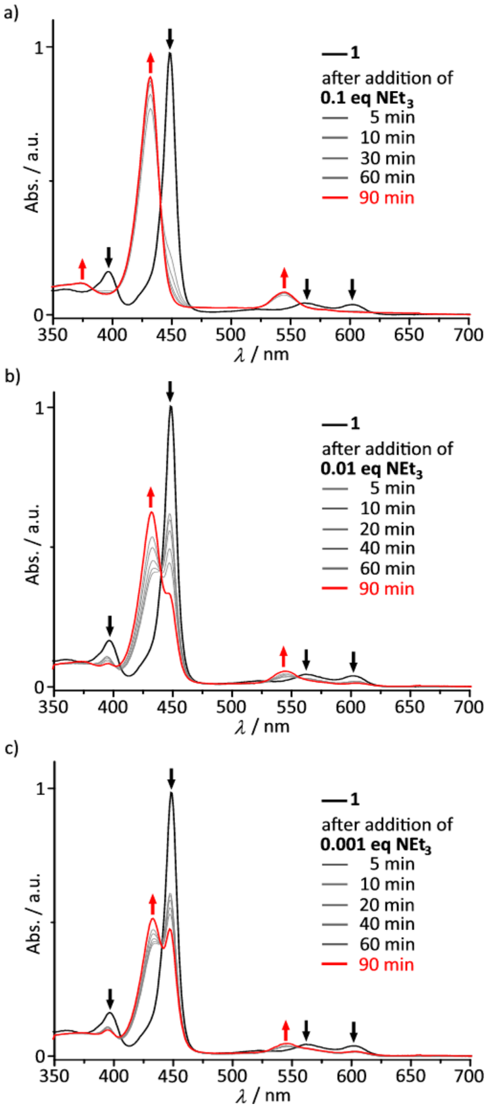

Figure 6. Temporal evolution of UV−vis absorption spectra of **1** in toluene after addition of (a) 0.1 equiv of NEt_3, (b) 0.01 equiv of NEt_3, and (c) 0.001 equiv of NEt_3. Red curves represent spectra after 90 min.

The kinetic traces suggest that the base-initialized pathway via $\mathbf{6}^-$ (early stages) proceeds faster than the chloride-initialized pathway via $\mathbf{5}^-$ (later stages, Figure 7). The slower reaction via intermediate $\mathbf{5}^-$ can either be ascribed to a less-favorable activation of **1** to form of $\mathbf{5}^-$ or a slower reaction of $\mathbf{5}^-$ with O_2.

Colorimetric Amine Sensing with 1. As **1** switches the color from green to red (Figure 1) upon exposure to nitrogenous bases with $pK_b \leq 3.2$, aqua complex **1** can be used as a simple colorimetric base indicator. Yet it shows distinct features distinguishing **1** from conventional colorimetric pH indicators. On the one hand the color change is

Scheme 4. Reaction Pathways of Inert 1 to 4 via Anionic Intermediates 5^- or 6^-

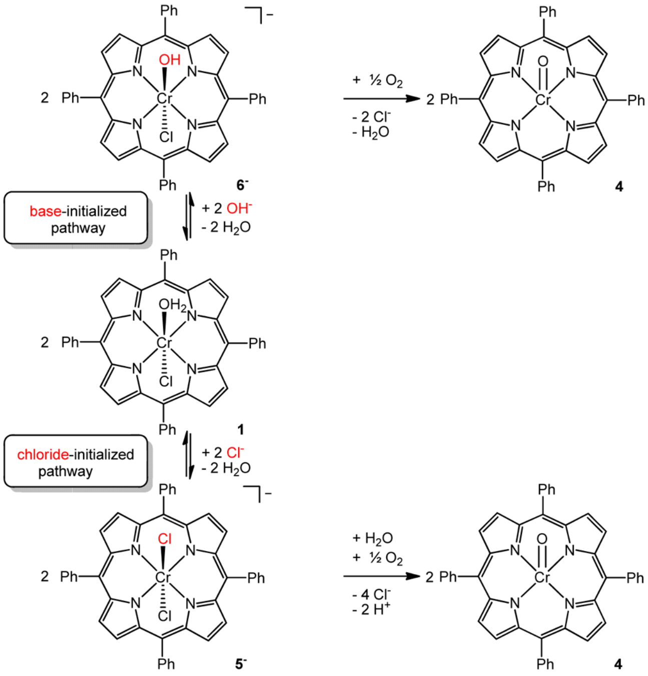

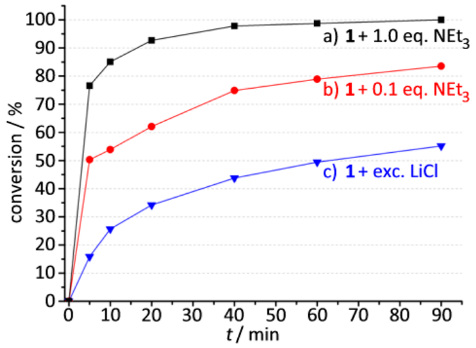

Figure 7. Kinetic traces of (a) **1** and 1 equiv of NEt_3 in CH_2Cl_2 (black), (b) **1** and 0.1 equiv of NEt_3 in CH_2Cl_2 (red), and (c) **1** and excess of LiCl in CH_2Cl_2 (blue) under ambient conditions.

irreversible. The initially reversibly formed species $\mathbf{6}^-/\mathbf{7}$ are subsequently oxidized irreversibly to form **4**, which is responsible for the observed red color. On the other hand even substoichiometric amounts of bases are detected with a full color change of the sensor, as the reaction is autocatalytically driven to completion by the released chloride (although slower). Sensor systems based on **1** can therefore be advantageously used for sensing applications that require a highly sensitive (amplified) ON response toward an analyte rather than quantification of the analyte via reversible binding.[55] Possible applications are the detection of toxic amine release into the environment or amine detection for the control of food freshness.[51−53] Because the detection event is easily visible to the human eye with its irreversible color change from green to red (Figure 1), the use of **1** or its derivatives leads to simple but powerful sensing devices.[26−28] As the chromium porphyrin chromophores can be successfully embedded in a suitable matrix[26−28] for gas-sensing devices, false positive signals resulting from adventitious Cl^- or OH^- are avoided, and only strong volatile amines will trigger the sensor to the ON state.

Dioxygen Activation with 1/Base. As epoxides are extremely valuable building blocks in synthetic organic chemistry a variety of protocols have been developed for the production of epoxides from olefins.[29] Essentially all protocols use oxidants such as hydroperoxides, peracids, hypochlorite, or iodosylbenzene.[29] Notable exceptions are the industrial aerobic epoxidation of ethane to ethylene oxide by an Al_2O_3-supported silver catalyst[56] and the aerobic epoxidation of olefins by Ru^{VI}(porphyrinato)$(O)_2$,[57a,b] Ru(salen)$(O)_n$ complexes,[57c] and a Ru^{IV}(6,6′-(SePh)-2,2′-bpy)$_2$$(O)_2$ complex[58] as well as a recently reported MOF based on Mn(salen) complexes.[59]

Epoxidation of olefins starting from **1** and MCPBA or iodosylbenzene/pentafluoro iodosylbenzene[34,60] as well as an electrochemically driven epoxidation using **4**[61,62] have been described before. In all cases reactive high-valent $[Cr^V(TPP)(O)]^+$ species ($\mathbf{4}^+$) are believed to be involved, although epoxidations with oxido chromium(V) complexes (in the gas phase) are shown to be formally spin-forbidden due to the different spin states of d^1 Cr^V (doublet) and d^3 Cr^{III} (quartet).[63]

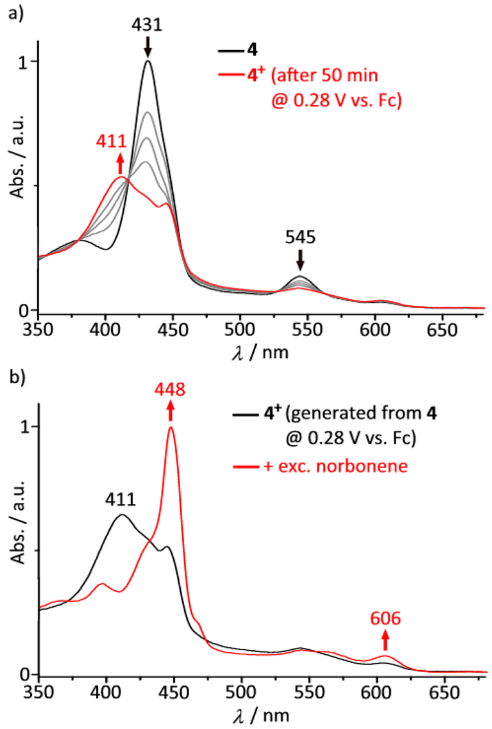

Figure 8. (a) Spectroelectrochemical oxidation of **4** in CH_2Cl_2/0.1 M $(^nBu_4N)(PF_6)$ and (b) UV−vis spectrum after subsequent addition of norbonene to $\mathbf{4}^+$.

We now have a clean pathway from **1** to **4** at hand by activation of **1** with bases and oxidation with O_2 instead of strong oxidants such as iodosylbenzene. Hence, the oxido chromium(IV) complex **4** prepared from **1**/LiOH/O_2 was employed in an electrochemical epoxidation of norbonene via single-electron oxidation of **4** to the reactive oxido chromium(V) porphyrin $\mathbf{4}^+$. Indeed, (spectro)electrochemical oxidation of **4** to $\mathbf{4}^+$ yields the Cr^V oxido complex, which is characterized by its Soret band at 411 nm with half of the original Soret band intensity as expected for $\mathbf{4}^+$ (Figure 8a).[31,64] An X-band EPR spectrum of this solution showed resonances at $g < 2.0$ expected for a d^1 Cr^V complex ($g_1 = 1.9865$, $g_2 = 1.9780$; 77 K;

CH_2Cl_2; Supporting Information, Figure S8).[64] Addition of norbonene caused the Soret band of 4^+ to disappear with concomitant appearance of the absorption bands of **1** similar to those reported in electrochemical studies (Figure 8b).[61,62] Finally, gas chromatography (GC) analysis of the solution from a bulk electrolysis of **4** in the presence of norbornene revealed the formation of *exo*-norbornene oxide during the course of the reaction by comparison with an authentic sample (see Supporting Information, Figures S9 and S10) similar to results reported in refs 61 and 62 starting from **4** prepared by conventional oxygenation of **1**. Oxidative electrolysis of **4** in the presence of excess norbonene yields the Cr^{III} complex **1** without accumulation of 4^+ according to spectroelectrochemical studies suggesting that the oxygen atom transfer to norbonene is comparably fast under these conditions (Supporting Information, Figure S11). Future studies will be devoted to optimizing the reaction conditions (base, porphyrin substituents,[65] dioxygen pressure, solvent, electrolyte), to exploring the substrate scope, and eventually to designing an electrocatalytic cycle using $\mathbf{1}/OH^-$ with O_2 as abundant, low-cost, and environmentally benign oxidant.[66−68]

CONCLUSION

In this study we disclosed the disjunctive mechanistic pathways of the reaction of different amines with the chromium(III) porphyrinato complex $Cr^{III}(TPP)(Cl)(H_2O)$ (**1**). Less basic amines L with $pK_b \geq 3.4$ act as Lewis bases substituting the aqua ligand to give green $Cr^{III}(TPP)(Cl)(L)$ complexes (**2**). However, amines with $pK_b \leq 3.2$ act as Brønsted bases deprotonating the aqua ligand to give the anionic hydroxido complex $[Cr^{III}(TPP)(Cl)(OH)]^-$ ($\mathbf{6}^-$). The latter is susceptible toward irreversible oxidation by dioxygen to the bright red oxido chromium(IV) complex $Cr^{IV}(TPP)(O)$ (**4**). Hence, **1** discriminates weakly and strongly basic amines by a distinct colorimetric green/red response. Furthermore, the activation/oxidation reaction sequence of the $\mathbf{1}$/amine/O_2 system is autocatalytic as **1** is also activated by chloride, which is stoichiometrically produced during the reaction. The irreversible formation of red **4** renders **1** a very sensitive amine-triggered ON switch, which is highly suitable for applications in food freshness control. The chromogenic signal is not only stable over time but also strongly amplified by the disclosed autocatalytic pathway. Furthermore, the green formation of the oxido chromium(IV) complex **4** by dioxygen (instead of hypochlorite, peracids, or iodosylbenzene) allows the use of this highly desirable oxidant for the (electrochemical) production of value-added products such as epoxides.

EXPERIMENTAL SECTION

Porphyrin complex **1** was prepared according to reported methods, and analytical properties conform with literature data.[1] Solvents and triethylamine for measurements under inert atmosphere were dried by standard methods and degassed by three pump−thaw cycles using argon. Other reagents were used as received from commercial suppliers (Sigma-Aldrich). UV−vis spectra were recorded on a Varian Cary 5000 spectrometer using 1.0 cm cells (Hellma, Suprasil). Samples for measurements under inert atmosphere were prepared in a glovebox and were measured in 1.0 cm quartz cells equipped with a Young valve. The NMR spectrum was recorded on a Bruker Avance DRX 400 spectrometer at 400.31 MHz (^1H). Resonances are reported in ppm versus the solvent signal as internal standard $CHCl_3$ (^1H: $\delta = 7.26$ ppm). Samples for mass spectrometry were dissolved in acetonitrile. FD mass spectra were recorded on an FD Finnigan MAT95 spectrometer. ESI mass spectra were recorded on a Micromass Q-TOF-Ultima spectrometer. Electrochemical experiments were carried out on a BioLogic SP-50 voltammetric analyzer using a glassy carbon working electrode, a platinum wire as a counter electrode, and a 0.01 M $Ag/AgNO_3$ electrode as a reference electrode. The measurements were carried out at a scan rate of 200 mV s^{-1} for cyclic voltammetry experiments and for square wave voltammetry experiments at negative potentials and of 100 mV s^{-1} for positive potentials. 0.1 M $(^nBu_4N)(PF_6)$ was used as a supporting electrolyte in CH_2Cl_2. Potentials are given relative to the ferrocene/ferrocenium redox couple ($E_{1/2}$ = 265 ± 5 mV under the experimental conditions). Spectroelectrochemical experiments were performed using a thin layer quartz glass (path length 1 mm) cell kit (GAMEC Analysentechnik, Illingen, Germany) equipped with a Pt gauze working electrode, a Pt counter electrode and a $Ag/AgNO_3$ reference electrode (10^{-5} M solutions in CH_2Cl_2 containing 0.1 M $(^nBu_4N)(PF_6)$). CW EPR spectra (X-band; ca. 9.4 GHz; ca. 20 mM) were measured on a Miniscope MS 300 at 298 K (Magnettech GmbH, Berlin, Germany). Settings were as follows: center field: 2499.01 G; modulation amplitude: 3000 mG; receiver gain: 5.0; microwave attenuation: 3 dB; sweep time: 120 s. *g* values are referenced to external Mn^{2+} in ZnS (g = 2.118, 2.066, 2.027, 1.986, 1.946, 1.906). Simulations of EPR spectra were performed with EasySpin (v 4.0.0)[69] for MatLab (R2007b). Bulk electrolysis of CH_2Cl_2 solutions containing **4** (4.6×10^{-4} M) and 100 equiv of *exo*-norbornene was performed in an electrochemical cell with two separated magnetically stirred compartments. The anode chamber was connected to the cathode chamber by a P2 glass filter membrane. A platinum mesh was used as anode, and a platinum wire was used as cathode. The $Ag/AgNO_3$ reference electrode was placed in the anode chamber. 0.5 M $(nBu_4N)(ClO_4)$ was used as the supporting electrolyte. The voltage was set to 0.48 V (vs Fc/Fc^+) for a period of 2 h. GC measurements were performed on a GC-2010 gas chromatograph (Shimadzu, Japan) equipped with a HP-5 silica capillary column (Agilent Technologies, USA; length 30 m, inner diameter: 0.25 mm, layer thickness of stationary phase: 0.5 μm) and a flame ionization detector. Carrier gas: hydrogen gas; temperature of injector: 250 °C; temperature of detector: 310 °C; column inlet pressure 64 kPa. Program: start temperature for 5 min: 30 °C; heating rate: 5 °C min^{-1}, end temperature: 100 °C.

Density Functional Calculations. These were carried out with the Gaussian09/DFT series[47] of programs. The B3LYP formulation of density functional theory was used employing the LANL2DZ basis set. No symmetry constraints were imposed on the molecules. The presence of energy minima of the ground states was checked by analytical frequency calculations. Solvent modeling was done employing the integral equation formalism polarizable continuum model (IEFPCM, dichloromethane). The approximate free energies at 298 K were obtained through thermochemical analysis of the frequency calculation, using the thermal correction to Gibbs free energy as reported by Gaussian09.

UV−vis Experiments Using 1. For all measurements 10^{-6} M solutions of **1** in CH_2Cl_2 or toluene were employed. This solution (3 mL) was transferred to a UV−vis cuvette to measure the initial UV−vis spectrum. For reactions with excess amines 10 μL of the respective neat amines were added. Excess LiCl was added in the form of 100 μL of a saturated solution in CH_2Cl_2. For experiments using 1.0, 0.1, 0.01, or 0.001 equiv solutions of NEt_3, LiOH or $CoCp^*_2$ (Cp* = pentamethylcyclopentadienyl) were prepared separately in the respective solvent with 100 μL containing the given equivalents. All cuvettes were shaken vigorously to ensure complete mixture before the measurements. Spectra recorded were numerically corrected for the respective concentration change by dilution.

UV−vis Experiments Using 8. A 10^{-6} M solution of **1** was prepared in dry THF and stirred with dry solid $CaCl_2$ under inert atmosphere for 30 min. An aliquot of this solution was transferred to a cuvette with a Young valve via a syringe equipped with a syringe filter. The UV−vis spectrum of this solution matches the literature data for **8**.[4] A further filtered aliquot was treated with excess dry NEt_3. The UV−vis spectrum of this solution remained unchanged. After 3 h the volatiles of this solution were removed under reduced pressure. The remaining solid was redissolved in CH_2Cl_2 under humid air, and excess NEt_3 was added. UV−vis spectra indicated the slow formation of **4**.

Characterization of 4. ^1H NMR: A sample of **1** in $CDCl_3$ was treated with excess of NEt_3 under air. The formation of **4** was monitored by UV−vis spectroscopy.[30,31] The solution was concentrated to give a concentration suitable for ^1H NMR spectroscopic analysis. ^1H NMR (400 MHz, $T = 298$ K): $\delta = 9.08$ (s, 8H, $CH^{pyrrole}$), 8.28 (br. s, 4 H, CH^{ortho}), 8.16 (br. s, 4 H, CH^{ortho}), 7.78 (br. s, 12 H, $CH^{meta,para}$).[31] For IR measurements a sample of **1** in CH_2Cl_2 was treated with LiOH/air, and the complete formation of **4** was checked by UV−vis spectroscopy prior to recording the IR spectrum of **4** in CH_2Cl_2. IR(CH_2Cl_2): $\tilde{\nu} = 1021$ (m, CrO), 998 (s) cm^{-1}.[31]

ASSOCIATED CONTENT

Supporting Information

Spectral characterization of **1**, **4**, and **4**$^+$; cyclic and square-wave voltammograms of **1** with/without addition of LiOH; UV−vis spectrum of the reaction of **1** with excess NH_3 in CH_2Cl_2; UV/vis spectra of **8** in THF, **8** in THF with exc. NEt_3, **8** in CH_2Cl_2 with exc. NEt_3 ; UV−vis spectra of the reaction of **1** with LiCl; X-band EPR spectrum of **4**$^+$; GC of the electrolysis solution of **4** and 100 equiv of norbonene; spectroelectrochemical oxidation of **4** in the presence of norbonene; Cartesian coordinates of all optimized structures. This material is available free of charge via the Internet at http://pubs.acs.org.

AUTHOR INFORMATION

Corresponding Author

*E-mail: katja.heinze@uni-mainz.de.

Author Contributions

The manuscript was written through contributions of all authors. All authors have given approval to the final version of the manuscript.

Notes

The authors declare no competing financial interest.

ACKNOWLEDGMENTS

We thank the Fonds National de la Recherche Luxembourg (FNR) for financial support through the "SurfAmine" project. We thank D. Schmitt, M. Mirion, S. Herold, and Prof. S. R. Waldvogel for assistance with the bulk electrolysis and the GC measurements.

REFERENCES

(1) Tsutsui, M.; Mitsuo, I.; Vohwinkel, F.; Keinosuke, S. *J. Am. Chem. Soc.* **1966**, *569*, 854−855.

(2) Tsutsui, M.; Velapoldi, R. A.; Suzuki, K.; Vohwinkel, F.; Ichikawa, M.; Koyano, T. *J. Am. Chem. Soc.* **1969**, *91*, 6262−6266.

(3) Adler, A. D.; Longo, F. R.; Kampas, F.; Kim, J. *J. Inorg. Nucl. Chem.* **1970**, *32*, 2443−2445.

(4) Summerville, D. A.; Jones, R. D.; Hoffmann, B. M.; Basolo, F. *J. Am. Chem. Soc.* **1977**, *99*, 8195−8202.

(5) Sanders, J. K. M.; Bampos, N.; Clyde-Watson, Z.; Darling, S. L.; Hawley, J. C.; Kim, H.-J.; Mak, C. C.; Webb, S. J. In *The Porphyrin Handbook;* Kadish, M.; Smith, K. M.; Guillard, R., Eds.; Academic Press: New York, 2000; Vol. 3, pp 1−48.

(6) Guldi, D. M.; Hambright, P.; Lexa, D.; Neta, P.; Savéant, J.-M. *J. Phys. Chem.* **1992**, *96*, 4459−4466.

(7) Bottomley, L. A.; Kadish, K. M. K. *Inorg. Chem.* **1983**, *22*, 342−349.

(8) Bottomley, L. A.; Kadish, K. M. *J. Chem. Soc., Chem. Commun.* **1981**, 1212−1214.

(9) More, K. M.; Eaton, G. R.; Eaton, S. S.; Hideg, K. *Inorg. Chem.* **1986**, *25*, 3865−3869.

(10) Harriman, A. *J. Chem. Soc., Faraday Trans. I* **1982**, *78*, 2727−2734.

(11) Gouterman, M.; Hanson, L. K.; Khalil, G.-E.; Leenstra, W. R.; Buchler, J. W. *J. Chem. Phys.* **1975**, *62*, 2343−2353.

(12) Ozawa, T.; Hanaki, A. *Inorg. Chim. Acta* **1985**, *102*, 169−171.

(13) Suslick, K. S.; Watson, R. A. *New J. Chem.* **1992**, *16*, 633−642.

(14) Inamo, M.; Hoshino, M.; Nakajima, K.; Aizawa, S.; Funahashi, S. *Bull. Chem. Soc. Jpn.* **1995**, *68*, 2293−2303.

(15) Fleischer, E. B.; Krishnamaurthy, M. *J. Am. Chem. Soc.* **1971**, *93*, 3784−3786.

(16) O'Brien, P.; Sweigart, D. A. *Inorg. Chem.* **1982**, *21*, 2094−2095.

(17) Inamo, M.; Sugiura, S.; Fukuyama, H.; Funahashi, S. *Bull. Chem. Soc. Jpn.* **1994**, *67*, 1848−1854.

(18) Inamo, M.; Hoshino, M. *Photochem. Photobiol.* **1999**, *70*, 596−601.

(19) Inamo, M.; Nakaba, H.; Nakajima, K.; Hoshino, M. *Inorg. Chem.* **2000**, *39*, 4417−4423.

(20) Heier, P.; Förster, C.; Schollmeyer, D.; Boscher, N.; Choquet, P.; Heinze, K. *Dalton Trans.* **2013**, *42*, 906−917.

(21) Pinto, S. M. A.; Lourenço, M. A. O.; Calvete, M. J. F.; Abreu, A. R.; Rosado, M. T. S.; Burrows, H. D.; Pereira, M. M. *Inorg. Chem.* **2011**, *50*, 7916−7918.

(22) Rakow, N. A.; Sen, A.; Janzen, M. C.; Ponder, J. B.; Suslick, K. S. *Angew. Chem.* **2005**, *117*, 4604−4608; *Angew. Chem., Int. Ed.* **2005**, *44*, 4528−4532.

(23) (a) Suslick, K. S.; Rakow, N. A.; Sen, A. *Tetrahedron* **2004**, *60*, 11133−11138. (b) Rakow, N. A.; Suslick, K. S. *Nature* **2000**, *406*, 710−713.

(24) Elisa, L.; Baldini, F.; Giannetti, A.; Trono, C.; Carofiglio, T. *Chem. Commun.* **2010**, *46*, 3678−3680.

(25) Anslyn, E. V. *J. Am. Chem. Soc.* **2010**, *132*, 15833−15835.

(26) Boscher, N. D.; Duday, D.; Heier, P.; Heinze, K.; Hilt, F.; Choquet, P. *Surf. Coat. Technol.* **2013**, *234*, 48−52.

(27) Boscher, N. D.; Bohn, T.; Heier, P.; Moisy, F.; Untereiner, B.; Heinze, K.; Choquet, P. *Sens. Actuators, B* **2014**, *191*, 553−560.

(28) Heier, P.; Bohn, T.; Choquet, P.; Boscher, N. D.; Heinze, K. *Adv. Funct. Mater.* **2014**, *2*, 1560−1570.

(29) *Mechanisms of homogeneous and heterogeneous epoxidation catalysis;* Oyama, S. T., Ed.; Elsevier B. V.: Amsterdam, The Netherlands, 2008.

(30) Liston, D. J.; West, B. O. *Inorg. Chem.* **1985**, *24*, 1568−1576.

(31) Groves, J. T.; Kruper, W. J.; Haushalter, R. C.; Butler, W. M. *Inorg. Chem.* **1982**, *21*, 1363−1368.

(32) Budge, J. R.; Gatehouse, B. M. K.; Nesbit, M. C.; West, B. O. *J. Chem. Soc., Chem. Commun.* **1981**, 370−371.

(33) Woo, L. K.; Hays, J. A.; Goll, J. G. *Inorg. Chem.* **1990**, *29*, 3916−3917.

(34) Groves, J. T.; Kruper, W. J., Jr. *J. Am. Chem. Soc.* **1979**, *101*, 7613−7615.

(35) Yuan, L. C.; Bruice, T. C. *J. Am. Chem. Soc.* **1985**, *107*, 512−513.

(36) Buchler, J. W.; Lay, K. L.; Ullrich, V. *Inorg. Chem.* **1982**, *21*, 842−844.

(37) Yuan, L.-C.; Calderwood, T. S.; Bruice, T. C. *J. Am. Chem. Soc.* **1985**, *107*, 8273−8274.

(38) (a) Meier-Callahan, A. E.; Gray, H. B.; Gross, Z. *Inorg. Chem.* **2000**, *39*, 3605−3607. (b) Meier-Callahan, A. E.; Di Bilio, A. J.; Simkhovich, L.; Mahammed, A.; Goldberg, I.; Gray, H. B.; Gross, Z. *Inorg. Chem.* **2001**, *40*, 6788−6793. (c) Mahammed, A.; Gray, H. B.; Meier-Callahan, A. E.; Gross, Z. *J. Am. Chem. Soc.* **2003**, *125*, 1162−1163. (d) Egorova, O. A.; Tsay, O. G.; Khatua, S.; Huh, J. O.; Churchill, D. G. *Inorg. Chem.* **2009**, *48*, 4634−4636. (e) Egorova, O. A.; Tsay, O. G.; Khatua, S.; Meka, B.; Maiti, N.; Kim, M. K.; Kwon, S. J.; Huh, J. O.; Bucella, D.; Kang, S. O.; Kwak, J.; Churchill, D. G. *Inorg. Chem.* **2010**, *49*, 502−512.

(39) Prokop, K. A.; Goldberg, D. P. *J. Am. Chem. Soc.* **2012**, *134*, 8014−8017.

(40) Fleischer, E. B.; Srivastava, T. S. *Inorg. Chim. Acta* **1971**, *5*, 151−154.

(41) Buchler, J. W.; Dreher, C.; Lay, K.-L.; Raap, A.; Gersonde, K. *Inorg. Chem.* **1983**, *22*, 879−884.

(42) Reed, C. A.; Kouba, J. A. Y. K.; Grimes, C. J.; Cheung, S. K. *Inorg. Chem.* **1978**, *17*, 2666−2670.

(43) Cheung, S. K.; Grimes, C. J.; Wong, J.; Reed, C. A. *J. Am. Chem. Soc.* **1976**, *98*, 5028−5030.

(44) Connelly, N. G.; Geiger, W. E. *Chem. Rev.* **1996**, *96*, 877−910.

(45) Koelle, U.; Infelta, P. P.; Grätzel, M. *Inorg. Chem.* **1988**, *27*, 879−883.

(46) Fuhrhop, J. H.; Kadish, K. M.; Davis, D. G. *J. Am. Chem. Soc.* **1973**, *95*, 5140−5147.

(47) Frisch, M. J.; Trucks, G. W.; Schlegel, H. B.; Scuseria, G. E.; Robb, M. A.; Cheeseman, J. R.; Scalmani, G.; Barone, V.; Mennucci, B.; Petersson, G. A.; Nakatsuji, H.; Caricato, M.; Li, X.; Hratchian, H. P.; Izmaylov, A. F.; Bloino, J.; Zheng, G.; Sonnenberg, J. L.; Hada, M.; Ehara, M.; Toyota, K.; Fukuda, R.; Hasegawa, J.; Ishida, M.; Nakajima, T.; Honda, Y.; Kitao, O.; Nakai, H.; Vreven, T.; Montgomery, Jr., J. A.; Peralta, J. E.; Ogliaro, F.; Bearpark, M.; Heyd, J. J.; Brothers, E.; Kudin, K. N.; Staroverov, V. N.; Kobayashi, R.; Normand, J.; Raghavachari, K.; Rendell, A.; Burant, J. C.; Iyengar, S. S.; Tomasi, J.; Cossi, M.; Rega, N.; Millam, J. M.; Klene, M.; Knox, J. E.; Cross, J. B.; Bakken, V.; Adamo, C.; Jaramillo, J.; Gomperts, R.; Stratmann, R. E.; Yazyev, O.; Austin, A. J.; Cammi, R.; Pomelli, C.; Ochterski, J. W.; Martin, R. L.; Morokuma, K.; Zakrzewski, V. G.; Voth, G. A.; Salvador, P.; Dannenberg, J. J.; Dapprich, S.; Daniels, A. D.; Farkas, Ö.; Foresman, J. B.; Ortiz, J. V.; Cioslowski, J.; Fox, D. J. *Gaussian 09,* Revision A.02; Gaussian, Inc.: Wallingford, CT, 2009.

(48) (a) Jentzen, W.; Ma, J.-G.; Shelnutt, J. A. *Biophys. J.* **1998**, *74*, 753−763. (b) Sun, L.; Shelnutt, J. A. *Normal-Coordinate Structural Decomposition Engine 3.0;* Sandia National Laboratories, 2001−2005. http://jasheln.unm.edu/jasheln/content/nsd/NSDengine/nsd_index.htm (accessed 9−15−2014).

(49) (a) Chrystiuk, E.; Williams, A. *J. Am. Chem. Soc.* **1987**, *109*, 3040−3046. (b) Hall, H. K. *J. Am. Chem. Soc.* **1957**, *79*, 5441−5444.

(50) Mcgrier, P. L.; Solntsev, K. M.; Miao, S.; Tolbert, L. M.; Miranda, O. R.; Rotello, V. M.; Bunz, U. H. F. *Chem.—Eur. J.* **2008**, *14*, 4503−4510.

(51) Xu, Y.; Xia, W.; Kim, J. M. *Int. J. Food Sci. Technol.* **2009**, *44*, 1547−1552.

(52) Balamatsia, C.; Patsias, A.; Kontominas, M.; Savvaidis, I. *Food Chem.* **2007**, *104*, 1622−1628.

(53) Veciana-Nogués, M. T.; Mariné-Font, A.; Vidal-Carou, M. C. *J. Agric. Food Chem.* **1997**, *45*, 2036−2041.

(54) Golovanov, I. B.; Zhenodarova, S. M. *Russ. J. Gen. Chem.* **2005**, *75*, 1795−1797.

(55) (a) Kumpf, J.; Bunz, U. H. F. *Chem.—Eur. J.* **2012**, *18*, 8921−8924. (b) Körsten, S.; Mohr, G. J. *Chem.—Eur. J.* **2011**, *17*, 969−975. (c) Lee, B.; Scopelliti, R.; Sverin, K. *Chem. Commun.* **2011**, *47*, 9639−9641. (d) Patze, C.; Broedner, K.; Rominger, F.; Trapp, O.; Bunz, U. H. F. *Chem.—Eur. J.* **2011**, *17*, 13720−13725. (e) Steiner, M.-S.; Meier, R. J.; Duerkop, A.; Wolfbeis, O. S. *Anal. Chem.* **2010**, *82*, 8402−8405. (f) Mohr, G. J. *Anal. Bioanal. Chem.* **2006**, *386*, 1201−1214. (g) Mohr, G. J.; Klimant, I.; Spichiger-Keller, U. E.; Wolfbeis, O. S. *Anal. Chem.* **2001**, *73*, 1053−1056. (h) Mohr, G. J.; Tirelli, N.; Lohse, C.; Spichiger-Keller, U. E. *Adv. Mater.* **1998**, *10*, 1353−1357.

(56) Kilty, P. A.; Sachtler, W. M. *Catal. Rev.: Sci. Eng.* **1974**, *10*, 1−16.

(57) (a) Groves, J. T.; Quinn, R. *J. Am. Chem. Soc.* **1985**, *107*, 5790−5792. (b) Lai, T.-S.; Zhang, R.; Cheung, K.-K.; Kwong, H.-L.; Che, C.-M. *Chem. Commun.* **1998**, 1583−1584. (c) Koya, S.; Nishioka, Y.; Mizoguchi, H.; Uchida, T.; Katsuki, T. *Angew. Chem.* **2012**, *124*, 8368−8371. *Angew. Chem., Int. Ed.* **2012**, *51*, 8243−8246.

(58) Laskavy, A.; Shimon, L. J. W.; Konstantinovski, L.; Iron, M. A.; Neumann, R. *J. Am. Chem. Soc.* **2010**, *132*, 517−523.

(59) Bhunia, A.; Gotthardt, M. A.; Yadav, M.; Gamer, M. T.; Eichhöfer, A.; Kleist, W.; Roesky, P. W. *Chem.—Eur. J.* **2013**, *19*, 1986−1995.

(60) Traylor, T. G.; Miksztal, A. R. *J. Am. Chem. Soc.* **1989**, *111*, 7443−7448.

(61) Creager, S. E.; Murray, R. W. *Inorg. Chem.* **1985**, *24*, 3824−3828.

(62) Garrison, J. M.; Bruice, T. C. *J. Am. Chem. Soc.* **1989**, *111*, 191−198.

(63) Crestoni, M. E.; Fornarini, S.; Lanucara, F.; Warren, J. J.; Mayer, J. M. *J. Am. Chem. Soc.* **2010**, *132*, 4336−4343.

(64) Groves, J. T.; Haushalter, R. C. *J. Chem. Soc., Chem. Commun.* **1981**, 1165−1166.

(65) (a) Melomedov, J.; Wünsche von Leupoldt, A.; Meister, M.; Laquai, F.; Heinze, K. *Dalton. Trans.* **2013**, *42*, 9727−9739. (b) Melomedov, J.; Ochsmann, J. R.; Meister, M.; Laquai, F.; Heinze, K. *Eur. J. Inorg. Chem.* **2014**, 1984−2001. (c) Melomedov, J.; Ochsmann, J. R.; Meister, M.; Laquai, F.; Heinze, K. *Eur. J. Inorg. Chem.* **2014**, 2902−2915.

(66) Punniyamurthy, T.; Velusamy, S.; Iqbal, J. *Chem. Rev.* **2005**, *105*, 2329−2363.

(67) Meunier, B. *Chem. Rev.* **1992**, *92*, 1411−1456.

(68) Tabushi, I. *Coord. Chem. Rev.* **1988**, *86*, 1−42.

(69) Stoll, S.; Schweiger, A. *J. Magn. Reson.* **2006**, *178*, 42−55.